ARTICLE
PUBLISHED ONLINE: 8 JUNE 2014 | DOI: 10.1038/NCHEMBIO.1554
nature chemical biology

Bioluminescent sensor proteins for point-of-care therapeutic drug monitoring

Rudolf Griss[1–3], Alberto Schena[1–3], Luc Reymond[1–3], Luc Patiny[1], Dominique Werner[4], Christine E Tinberg[5], David Baker[5] & Kai Johnsson[1–3]*

For many drugs, finding the balance between efficacy and toxicity requires monitoring their concentrations in the patient's blood. Quantifying drug levels at the bedside or at home would have advantages in terms of therapeutic outcome and convenience, but current techniques require the setting of a diagnostic laboratory. We have developed semisynthetic bioluminescent sensors that permit precise measurements of drug concentrations in patient samples by spotting minimal volumes on paper and recording the signal using a simple point-and-shoot camera. Our sensors have a modular design consisting of a protein-based and a synthetic part and can be engineered to selectively recognize a wide range of drugs, including immunosuppressants, antiepileptics, anticancer agents and antiarrhythmics. This low-cost point-of-care method could make therapies safer, increase the convenience of doctors and patients and make therapeutic drug monitoring available in regions with poor infrastructure.

Drug dosage needs to strike a balance between efficacy and toxicity. Many immunosuppressants, antiepileptics, antibiotics and other drugs have unpredictable pharmacokinetics and narrow therapeutic ranges, requiring monitoring of their concentrations in the body. This process, known as therapeutic drug monitoring (TDM), currently relies on immunoassays and chromatographic techniques, but such methods require dedicated personnel and infrastructure[1]. Although measuring blood glucose levels at the point of care is well established, low-cost methods for quantifying drug levels are still lacking. The development of fast and low-cost assays would improve safety and therapeutic outcome in regions with poor infrastructure and allow personalized dosage at bedside or at home.

Moving TDM from the diagnostic lab to the patient requires tools that (i) are capable of handling minimal sample volumes down to a single drop, (ii) are quantitative, (iii) do not require operator intervention and (iv) permit automated readout with inexpensive, portable devices. We introduce here luciferase-based indicators of drugs (LUCIDs), a new class of biosensors that fulfill all of these demands.

LUCIDs are ratiometric, bioluminescent sensor proteins made up of three components: a receptor protein for the drug of interest, a luciferase and a synthetic molecule containing a fluorophore and a ligand for the receptor protein (**Fig. 1a**,**b**). The attached ligand binds in an intramolecular manner to the receptor protein, bringing the fluorophore close to the luciferase and permitting efficient bioluminescent resonance energy transfer (BRET). Sufficient concentrations of analyte can displace the ligand from the receptor protein, causing BRET efficiency to decrease. Recording the ratio of light emitted from the luciferase (blue) and the synthetic fluorophore (red) permits quantification of the concentration of the analyte independently of sensor concentration and signal intensity. We have previously shown that competition between a tethered ligand and free analyte permits the design of Förster resonance energy transfer (FRET)-based sensor proteins[2–5], but the use of bioluminescence simplifies the readout, increases sensitivity and renders the sensor protein independent from external light sources—important features for the development of point-of-care devices.

RESULTS

Sensor development

As a first analyte, we chose the anticancer agent methotrexate (**Fig. 1**). High drug concentrations are required to kill tumor cells, and TDM is required to prevent excessive toxicity by guiding dose adjustment of folinic acid[6]. To create a LUCID for methotrexate, we chose bacterial dihydrofolate reductase (DHFR) as a receptor protein and the DHFR inhibitor trimethoprim as an intramolecular ligand. The sensor then is a fusion protein of DHFR, the luciferase NanoLuc and SNAP-tag[7] for the specific attachment of the synthetic molecule containing the fluorophore Cy3 and trimethoprim (**Fig. 1a**,**b**). We inserted a rigid 30-proline linker between SNAP-tag and NanoLuc to push the fluorophore and the luciferase apart, ensuring low BRET efficiency in the open state of the sensor. Titration of this sensor with methotrexate revealed a maximum ratio change of 218 ± 6% (± s.d.) (**Supplementary Results**, **Supplementary Fig. 3**). Even though this is the highest dynamic range for any BRET biosensor reported so far[8], we speculated that we could improve it by bringing the luciferase closer to the active site of DHFR and thus to the acceptor fluorophore in the closed state of the sensor. We constructed a circularly permuted DHFR variant, moving the N terminus to residue Asn23, which is located in a loop next to the protein's active site (**Fig. 1c**)[9]. This increased the sensor's ratio change more than sixfold to 1,340 ± 90% (**Fig. 1d**,**e**). Titrating the sensor with increasing concentrations of methotrexate permitted us to determine the concentration resulting in 50% of the maximum ratio change (c_{50}) of 0.75 ± 0.04 μM. An attractive feature of the sensor design is that we can adjust the c_{50} for a given drug by changing the affinity of the tethered ligand. For example, replacing trimethoprim by the stronger inhibitor methotrexate shifts the c_{50} of the sensor from 0.75 ± 0.04 μM to 85 ± 6 μM (**Fig. 1e**). Together,

[1]École Polytechnique Fédérale de Lausanne, Institute of Chemical Sciences and Engineering, Lausanne, Switzerland. [2]École Polytechnique Fédérale de Lausanne, Institute of Bioengineering, Lausanne, Switzerland. [3]National Centre of Competence in Research in Chemical Biology, Lausanne, Switzerland. [4]Clinical Chemistry Laboratory, Service of Biomedicine, Centre Hospitalier Universitaire Vaudois (CHUV), Lausanne, Switzerland. [5]University of Washington, Department of Biochemistry, Seattle, Washington, USA. *e-mail: kai.johnsson@epfl.ch

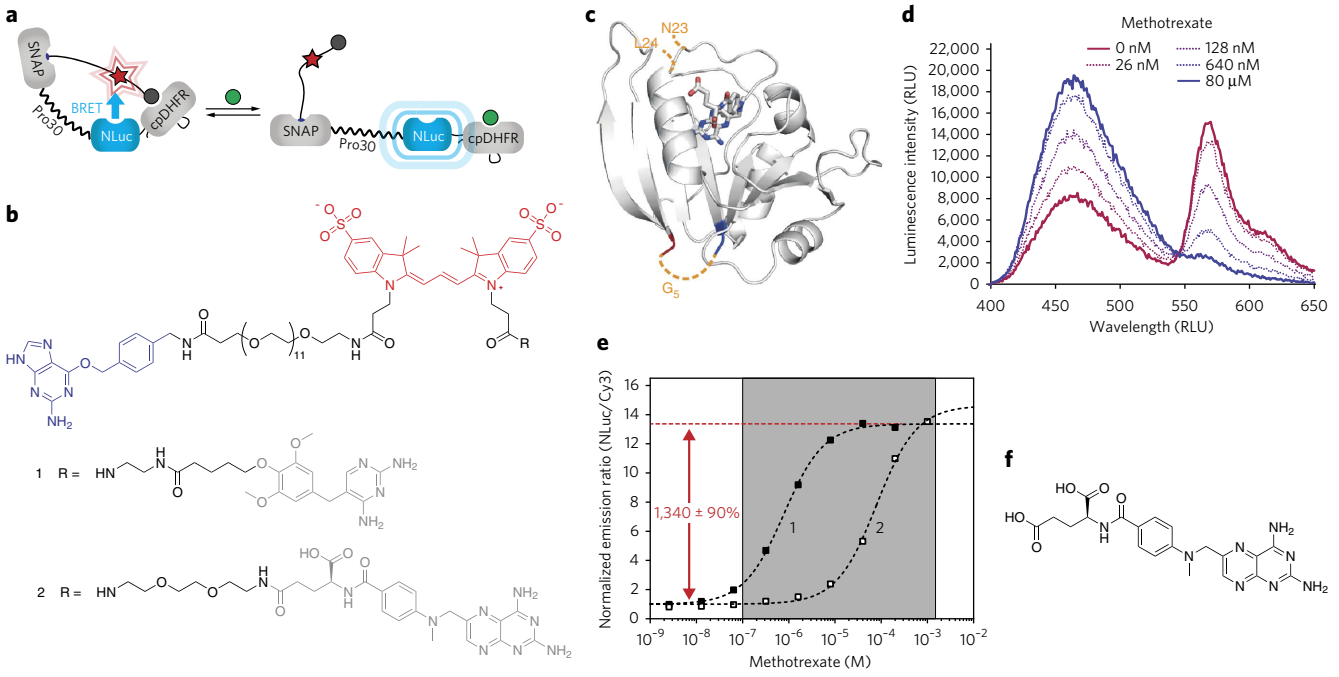

Figure 1 | Design and performance of a sensor for methotrexate. (**a**) The fusion protein SNAP-Pro30-NanoLuc (NLuc)-cpDHFR is linked to a synthetic molecule containing a fluorophore (red star) and a DHFR inhibitor (gray ball). Free analyte (green ball) can shift the sensor to an open conformation, reducing BRET efficiency. (**b**) Structure of the synthetic molecules used to assemble the sensor. The benzylguanine group (blue) serves as the reactive moiety for SNAP-tag labeling, the fluorophore Cy3 is colored in red, and the tethered DHFR inhibitors trimethoprim (BG-Cy3-TMP; **1**) and methotrexate (BG-Cy3-MTX; **2**) are shown in gray. (**c**) Structure of *E. coli* DHFR bound to methotrexate[24]. The N terminus is shown in blue, the C terminus is shown in red, and the position of the new termini produced by circular permutation (N23 and L24) as well as the 5-glycine linker used to connect the original termini are shown in orange. (**d**) Emission spectra of SNAP-Pro30-NanoLuc-DHFRcpL24G5 labeled with BG-Cy3-TMP (**1**) in human serum spiked with defined concentrations of methotrexate. RLU, relative luminescence units. (**e**) The sensor protein labeled with BG-Cy3-TMP (**1**) has a ratio change of 1,340 ± 90% and a c_{50} of 0.75 ± 0.04 µM (obtained from three independent titrations; the graph shows one titration). The sensor protein labeled with BG-Cy3-MTX (**2**) has a c_{50} of 85 ± 6 µM (obtained from three titrations; the graph shows one titration). Error represents s.d. (**f**) Chemical structure of methotrexate.

the two constructed sensors permit the measurement of methotrexate serum concentrations from 100 nM to 1.5 mM, covering most of the range of methotrexate concentrations as they occur during therapy[10]. The metabolites 7-hydroxy methotrexate and 4-amino-4-deoxy-*N*-methylpteroic acid (DAMPA), which interfere with existing immunoassays[11], have c_{50} values that are at least two orders of magnitude higher than that of methotrexate and thus do not affect measurements (**Supplementary Fig. 4**).

Measurements in human samples using a digital camera

To use LUCIDs for quantifying drug concentrations in human samples, they need to be insensitive to matrix effects. However, light-absorbing molecules can distort the measured emission intensity ratio. For example, the serum component bilirubin strongly absorbs blue light, and its concentration can vary substantially between human samples (normal levels are 5.1–17.0 µM)[12]. We found that adding an additional 10 µM bilirubin to commercial human serum markedly changes the measured BRET intensity ratios (**Supplementary Fig. 5a**). We speculated that reducing the distance emitted light has to travel through the serum could solve this problem. To spread out samples as a thin layer, we spotted them on chromatography paper and analyzed the emitted light. Under such conditions, the measured emission intensity ratio became independent of bilirubin concentrations (**Supplementary Fig. 5b**).

We did all of the above measurements using a traditional microplate reader, which is not compatible with point-of-care applications. As the emission peaks of NanoLuc and Cy3 are well separated and overlap with the blue and red color channels of standard complementary metal-oxide-semiconductor (CMOS) and charge-coupled device (CCD) image sensors, we investigated whether sample analysis could be achieved with simple digital cameras. We spotted 5 µl of human serum containing 50 nM LUCID and varying concentrations of methotrexate onto chromatography paper patterned with wax rings that confine the applied solution within their borders (**Fig. 2a**). Standard printers can easily produce such patterns[13]. We placed the paper into a simple polystyrene icebox to exclude surrounding light and took a picture with a digital camera (costing <$100) through a hole in the box (**Fig. 2a**). We could clearly detect glowing spots and observed a methotrexate-dependent color transition from red to blue. We quantified the signal using a software script that recognizes the spots, determines the average intensity per pixel in the blue and red color channels and calculates their ratio (**Fig. 2b**). Using such a portable detection device, which anybody can easily assemble from any cardboard box and a simple digital camera in about 10 min, we could measure titration curves not only in serum but also in strongly absorbing whole blood (**Supplementary Figs. 6** and **7**).

Using our point of care–compatible prototype, we quantified methotrexate concentrations in 30 patient samples and compared the results to those obtained by a standard fluorescence polarization immunoassay. We observed a very good correlation between the results obtained with the two different methods (**Fig. 2c** and **Supplementary Fig. 8**). Our LUCID also displayed a good reproducibility with an average interassay coefficient of variation of 16%. The excellent performance of our simple, homemade device clearly demonstrates the potential of LUCIDs for point-of-care TDM.

Engineering LUCIDs for different analytes

To demonstrate the generality of our approach, we developed additional LUCIDs for five commonly monitored drugs: the

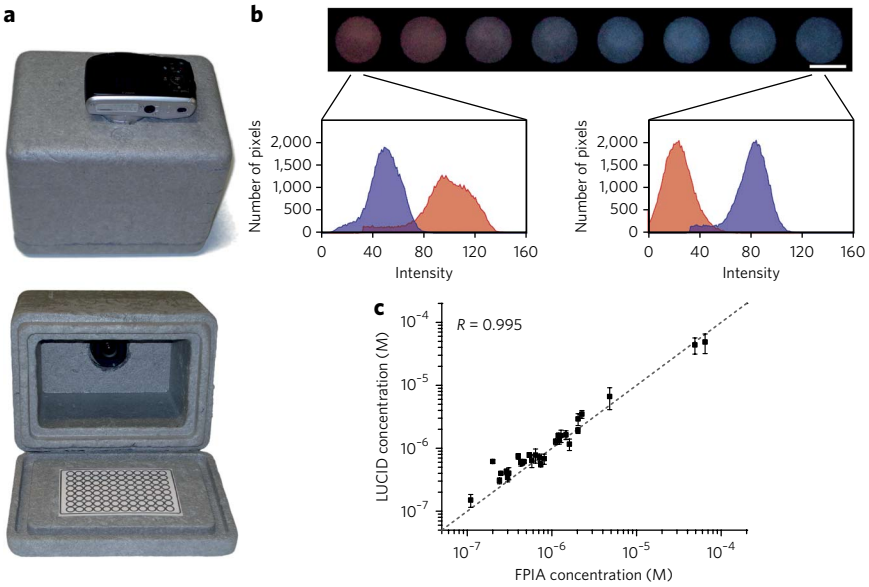

Figure 2 | Measuring methotrexate concentrations in patient samples using a point-and-shoot digital camera. (**a**) Pictures of the box and camera used for detection. The chromatography paper with printed wax circles can be seen in the bottom picture. (**b**) Picture of spotted SNAP-Pro30-NanoLuc-DHFRcpL24G5 labeled with BG-Cy3-TMP with varying methotrexate concentrations in human serum taken with a digital camera. Scale bar, 5 mm. The histograms show the intensity distributions of pixels in the red and blue channels. (**c**) Correlation of the results obtained for patient serum samples using LUCIDs and a traditional fluorescence polarization immunoassay. Each LUCID measurement is given as the mean ± s.d. of three independent measurements. Regression analysis yielded a Pearson correlation coefficient (R) = 0.995. The two samples highest in concentration were diluted tenfold in commercial human serum before the measurement.

immunosuppressants tacrolimus and sirolimus (**Fig. 3**) as well as cyclosporin A (**Fig. 4**), the antiepileptic topiramate and cardiac glycoside digoxin (**Fig. 5**).

The macrolide tacrolimus is one of the most widely used immunosuppressants. Its variable pharmacokinetics, combined with the need for maintaining a narrow therapeutic range to prevent toxicity without risking transplant rejection, requires TDM[14]. We chose the target of tacrolimus, FKBP12, as a receptor protein. However, this protein is geometrically not well suited for obtaining a high BRET efficiency in the closed state of the sensor. Both termini lie far away from the active site, and the distance between them is large, excluding circular permutation as a viable strategy (**Fig. 3a**). Moreover, the concentrations of tacrolimus in blood during therapy are low (6–19 nM)[14], making it necessary to have a weak intramolecular ligand that can be easily displaced. Recently, bipartite ligands for FKBP12 have been described that, in addition to the protein's active site, bind a secondary site close to the N terminus[15] (**Fig. 3a**,**b**). Those parts of the ligands that only bind the secondary site have affinities of around 100 µM and would thus be too weak to close the sensor completely in the absence of analyte. On the basis

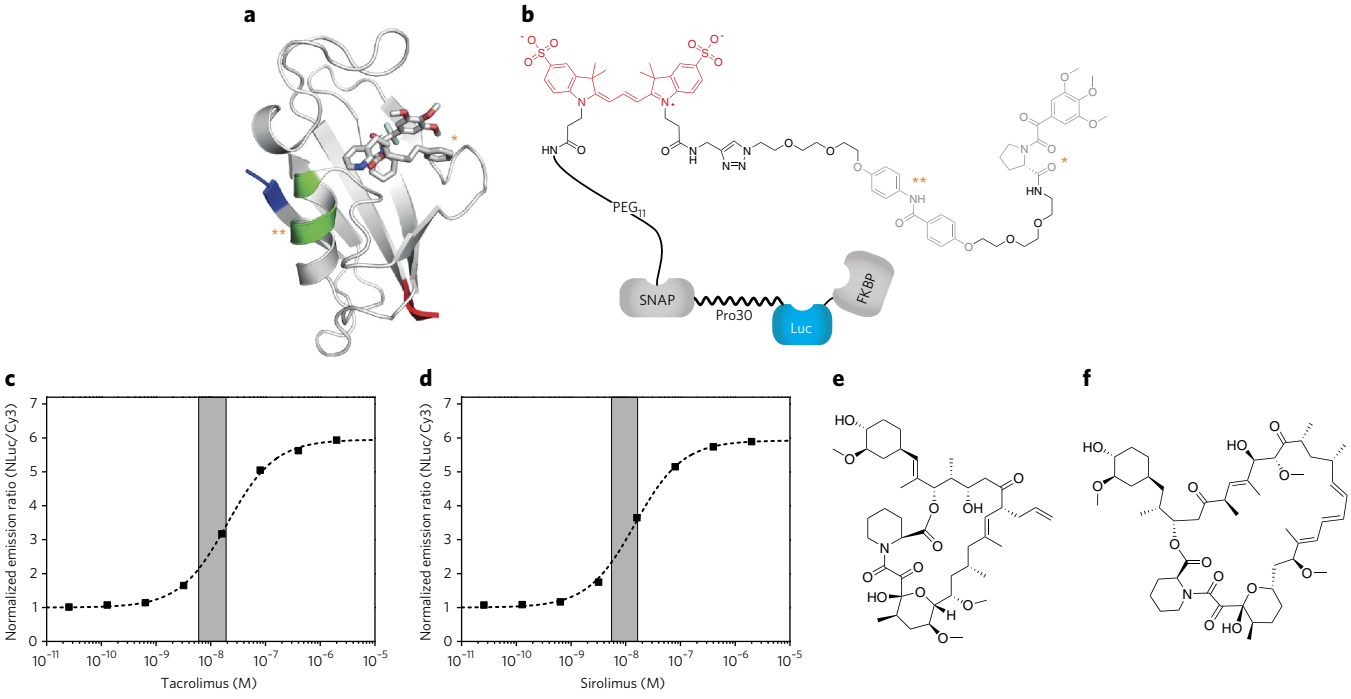

Figure 3 | LUCID for tacrolimus and sirolimus. (**a**) Crystal structure of FKBP12 bound to an inhibitor that occupies the primary binding site (orange asterisk)[25]. The secondary binding site is shown in green (two orange asterisks). The N terminus is shown in blue, and the C terminus is shown in red. (**b**) Design of the sensor. The parts of the ligand that target the different binding sites on FKBP12 are marked with orange asterisks. (**c**) Titration of the sensor with tacrolimus yielded a ratio change of 460 ± 30% and a c_{50} of 17 ± 3 nM (obtained from three independent titrations; the graph shows one titration). Error represents s.d. The shaded area corresponds to the therapeutic range of the drug. (**d**) Titration of the sensor with sirolimus gave a ratio change of 480 ± 30% and a c_{50} of 13.7 ± 1.6 nM (obtained from three independent titrations; the graph shows one titration). The shaded area corresponds to the therapeutic range of the drug (5.5–16.5 nM)[26]. (**e**) Chemical structure of tacrolimus. (**f**) Chemical structure of sirolimus.

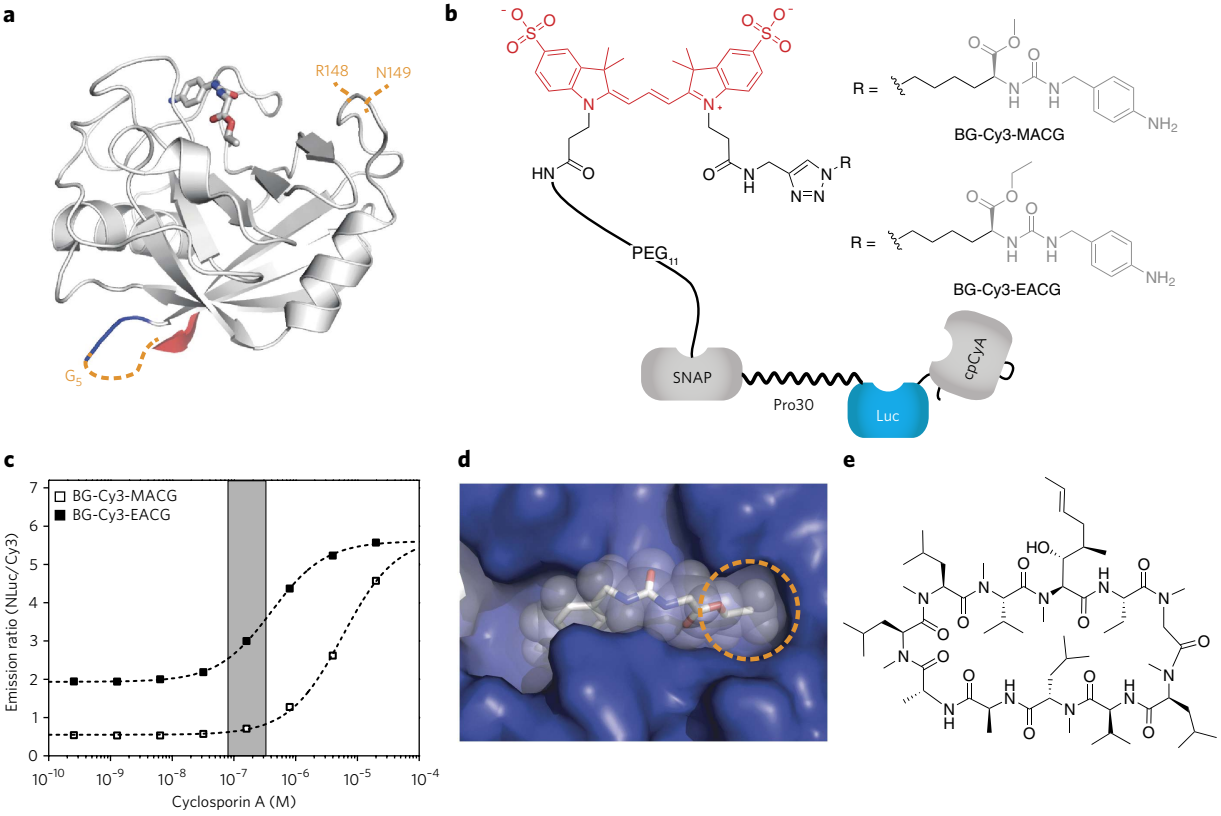

Figure 4 | LUCID for cyclosporin A. (**a**) Crystal structure of cyclophilin A bound to the inhibitor EACG (PDB ID 3RDD). The N terminus is shown in blue, the C terminus is shown in red, and the position of the new termini produced by circular permutation (R148 and N149) and the 5-glycine linker used to connect the original termini are shown in orange. (**b**) Design of the sensor with the reported cyclophilin A inhibitor EACG and the designed inhibitor MACG. (**c**) Titration of the sensor containing the two different intramolecular inhibitors with cyclosporin A. For BG-Cy3-MACG, we obtained a ratio change of 192 ± 5% and a c_{50} of 500 ± 90 nM; for BG-Cy3-EACG we obtained a ratio change of 900 ± 30% and a c_{50} of 5.9 ± 1.4 μM (obtained from three independent titrations; the graph shows one titration). Error represents s.d. The shaded area corresponds to the therapeutic range of the drug. Although the emission ratios at high analyte concentrations are similar, the weaker inhibitor does not reach the ratio of the fully closed sensor in the absence of analyte. However, with the stronger inhibitor, the c_{50} is too high for measuring cyclosporin A in its therapeutic range. (**d**) Rationale for ligand design: the crystal structure of EACG bound to cyclophilin A shows that the ethyl group of the ester points into a hydrophobic pocket (PDB code 3RDD). (**e**) Chemical structure of cyclosporin A.

of published results[15], we designed a ligand that spans both binding sites on FKBP12 and that should have an affinity around 1 μM. We attached the fluorophore Cy3 to the part of the ligand that upon binding should be close to the N terminus of the protein (**Fig. 3b**). The resulting LUCID displays a BRET ratio change of 460 ± 30% and a c_{50} of 17 ± 3 nM (**Fig. 3c**). This c_{50} value is in the range of tacrolimus concentrations found in blood during therapy. Moreover, we can also use the sensor for TDM of the important immunosuppressive sirolimus, which binds the same receptor protein (**Fig. 3d**). As for the LUCID for methotrexate, we can read out the signal of this sensor using a digital camera (**Supplementary Fig. 13a,b**).

Cyclosporin A is another important immunosuppressant for which TDM is indispensable[14]. We chose the drug's target, human cyclophilin A, as a receptor protein. As the protein's termini do not lie close to its active site, we decided to follow a similar strategy as for DHFR. We found that residues Arg148 and Asn149 are poorly conserved between variants from different species and speculated that they are not important for the protein's structure and function. Moreover, the two amino acids reside in a loop close to the binding site. For these reasons, we constructed a cyclophilin A mutant that is circularly permuted between residues Arg148 and Asn149, connecting the original termini by a 5-glycine linker and producing new termini in close proximity to the active site (**Fig. 4a** and **Supplementary Fig. 9**). As cyclosporin A concentrations during therapy are rather low (83–333 nM)[12], we had to choose a weak inhibitor as intramolecular ligand. We first attempted to use the recently described cyclophilin A inhibitor ethyl ((4-aminobenzyl) carbamoyl)glycinate (Protein Data Bank (PDB) code 3RDD) but obtained a c_{50} for cyclosporine of > 5 μM (**Fig. 4b,c**). The crystal structure of the inhibitor bound to its target reveals that the ethyl group of the ester makes important hydrophobic contacts with the protein (**Fig. 4d**). We speculated that replacing the ethyl by a methyl group should lower the affinity of the intramolecular ligand. The resulting ligand was too weak to close the sensor completely in the absence of analyte, leading to the slightly lower BRET ratio change of 192 ± 5%. However, as expected, the LUCID's response was shifted to a c_{50} of 500 ± 90 nM, making it suitable for TDM of the drug (**Fig. 4c**). As for the other LUCIDs, we were also able to use a digital camera for readout (**Supplementary Fig. 13c**).

The antiepileptic topiramate is widely used for the prevention of seizures in epilepsy. Optimizing the dose is critical, but the prophylactic nature of the drug prevents physicians from finding sufficient doses quickly without missing the subtle signs of toxicity[16]. Using TDM, doctors can adjust the dose to maintain effective but subtoxic drug serum concentrations. Topiramate is an inhibitor of human carbonic anhydrase II (HCA), and we chose HCA as the receptor protein for the generation of a LUCID for topiramate (**Fig. 5a,b**). We previously used HCA as a receptor protein and benzene sulfonamides as intramolecular ligands for the generation of a FRET-based sensor[2,4]. However, to achieve a response of an HCA-based LUCID at clinically relevant topiramate concentrations, we needed to generate benzene sulfonamides with lower affinity toward HCA than those previously

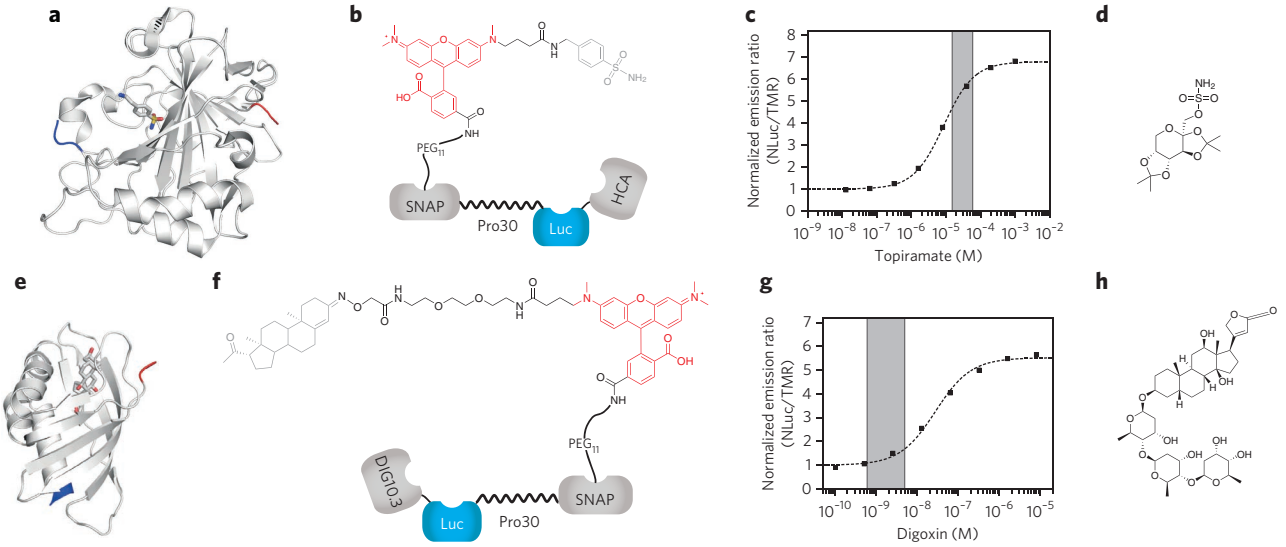

Figure 5 | LUCIDs for topiramate and digoxin. (**a**) Crystal structure of HCA bound to a sulfonamide inhibitor[27]. The N terminus is shown in blue and the C terminus is shown in red. (**b**) Design of the LUCID for topiramate. (**c**) Titration of the sensor with topiramate gives a ratio change of 591 ± 12% and a c_{50} of 7.3 ± 1.3 μM (obtained from three independent titrations; the graph shows one titration). Error represents s.d. The shaded area corresponds to the therapeutic range of the drug. (**d**) Chemical structure of topiramate. (**e**) Crystal structure of DIG10.3 bound to digoxigenin[19]. The N terminus is shown in blue, and the C terminus is shown in red. (**f**) Design of the LUCID for digoxin. (**g**) Titration of the sensor with digoxin gives a ratio change of 458 ± 11% and a c_{50} of 22 ± 5 nM (obtained from three independent titrations; the graph shows one titration). Error represents s.d. The shaded area corresponds to the therapeutic range of the drug. (**h**) Chemical structure of digoxin.

used (**Supplementary Fig. 10**). The resulting LUCID can detect topiramate with a ratio change of 591 ± 12% and a c_{50} of 7.3 ± 1.3 μM (**Fig. 5c**), and we can read it out using a digital camera (**Supplementary Fig. 13d**). These properties make it highly suitable for measuring the drug in its therapeutic range (15–60 μM)[16]. It should also be noted that in this LUCID we used a tetramethylrhodamine derivative as BRET acceptor as it resulted in a higher ratio change than the corresponding Cy3 derivative (**Supplementary Fig. 11**).

Digoxin is a widely used drug for the treatment of heart conditions. As the therapeutic window is small and symptoms arising from drug toxicity are difficult to distinguish from the clinical symptoms of the treated condition, TDM is necessary[17]. The protein target of digoxin is a (Na^+-K^+)-ATPase membrane pump[18], and such an integral membrane protein is not a suitable receptor for our sensor design. Recently, a computationally designed high-affinity binding protein for digoxin, DIG10.3, has been described[19]. The therapeutic levels of digoxin in serum are extremely low (0.6–2.5 nM)[20], requiring an intramolecular ligand with low affinity. We chose progesterone, which binds weakly to DIG10.3 and should thus be displaced easily by low digoxin concentrations. As the C but not the N terminus of DIG10.3 lies in close proximity to its binding site, we inverted the geometry of the fusion protein to obtain DIG10.3-NanoLuc-Pro30-SNAP (**Fig. 5e**,**f** and **Supplementary Fig. 12**). This brings the fluorophore into close proximity of the luciferase in the closed state of the sensor, leading to a high BRET efficiency. The sensor displays a BRET ratio change of 458 ± 11% and a c_{50} of 22 ± 5 nM for digoxin in human serum (**Fig. 5g**), and we can read it out using a digital camera (**Supplementary Fig. 13e**). The c_{50} of this digoxin LUCID is too high to measure the drug at its low therapeutic levels but is suitable to detect toxic levels exceeding 5 nM (ref. 21). More importantly, this example demonstrates that computational protein design extends the range of analytes for which LUCIDs can be generated to those for which no appropriate natural binding protein is available.

DISCUSSION

An important step toward personalized medicine will be to decentralize diagnostics and move them from the lab to the patient. This trend brings benefits to the individual patient as well as to society as a whole, increasing convenience, improving therapies and reducing healthcare costs. In the same way that people are starting to use their smartphones to monitor their fitness, they will in the future be able to measure biochemical parameters and monitor their health state wherever they are. To date, only electrochemical biosensors such as the glucose meter are successfully used for quantitative measurements at the point of care. The development of sensors for other analytes is an active area of research[22], but very few have made it to the market. LUCIDs introduce an entirely new mechanism for inexpensive point-of-care biosensors. They are to our knowledge the first sensor proteins that exploit the light-emitting properties of luciferases to accurately quantify the concentrations of analytes in patient samples. A drop of the sample is simply spotted onto a piece of filter paper, and the emitted light is analyzed with a basic digital camera. Potential problems arising from the variable composition of samples are avoided. We have demonstrated the generality of our approach: through a combination of protein engineering and ligand design, sensor proteins for virtually any analyte can be constructed. Their simplicity and versatility make LUCIDs ideally suited for home use and point of care-applications.

Two aspects are crucial for constructing a LUCID for any new analyte: the engineering of the binding protein and the ligand design. The geometry of the binding protein is key to achieving a high ratio change. Rigid polyproline linkers between SNAP-tag and the luciferase can reliably bring the BRET efficiency in the sensor's open state to a minimum. To obtain a high BRET efficiency in the closed state, the luciferase's point of attachment has to be in close proximity to the binding pocket of the binding protein. In cases where none of the two termini are suitable, circular permutation has proven to be a viable strategy to move the termini to a desired position.

The ligand design is important for tuning the equilibrium between the open and closed sensor states. The sensor response can be viewed as a two-step process: the unbinding of the tethered ligand followed by the binding of the analyte. In the absence of analyte, the ratio of open and closed sensor molecules is equal to the affinity of the tethered ligand divided by its effective molarity[23]. From our

previous studies of similar sensor systems, we estimate the effective molarity to be around 100 µM (ref. 2). In the absence of analyte, the affinity of the intramolecular ligand thus has to be lower than 10 µM for the sensor's closed state to be favored at least tenfold over its open state. The fact that such moderate affinities are sufficient is an important advantage over intermolecular displacement assays. Moreover, because the c_{50} for a given drug is inversely proportional to the affinity of the tethered ligand, the sensor response can be tuned to the therapeutically most relevant concentration range.

One of the key parameters of any ratiometric biosensor is its maximum ratio change. LUCIDs are the first BRET-based sensors that can quantify small molecules with truly high ratio changes, clearly surpassing the ratio change of any previously reported BRET-based indicator[8]. They introduce both a new sensor mechanism and a new type of readout for diagnostics and might well be combined with current trends in the field such as the use of microfluidics or multiplexing.

Several steps still need to be taken to take LUCIDs from the proof-of-concept stage to a device that can be used in practice. We foresee a setup in which the protein and the luciferase substrate are dried on separate layers of paper and a membrane is used on top of them to filter out the red blood cells, as it has been previously done[13]. The patient would prick his or her finger and transfer a drop of blood onto the membrane, and the serum would diffuse into the paper containing the luciferase substrate and the sensor protein. A handheld device could then read the produced light from the opposite side. This instrument only needs to quantify the intensity of blue and red light; a whole camera, as used in this study, will therefore not be necessary. The device should automatically calculate the analyte concentration on the basis of the intensity of blue and red light and have a user interface, which is easy to use for both doctors and patients. The stability of the sensor protein and the luciferase substrate, when dried on paper, will have to be evaluated and potentially optimized. However, it has been previously shown that proteins can be stable for long periods of time in this state[13].

In conclusion, LUCIDs are a family of semisynthetic, bioluminescent sensor proteins that through protein engineering and ligand design can be constructed to recognize diverse analytes. They permit the quantitative analysis of patient samples with simple, portable devices. By making TDM more easily accessible, LUCIDs could not only improve patient care in developed areas but also bring its benefits to regions with poor infrastructure.

Received 30 January 2014; accepted 15 May 2014;
published online 8 June 2014

METHODS

Methods and any associated references are available in the online version of the paper.

References

1. Saint-Marcoux, F., Sauvage, F.L. & Marquet, P. Current role of LC-MS in therapeutic drug monitoring. *Anal. Bioanal. Chem.* **388**, 1327–1349 (2007).
2. Brun, M.A., Tan, K.T., Nakata, E., Hinner, M.J. & Johnsson, K. Semisynthetic fluorescent sensor proteins based on self-labeling protein tags. *J. Am. Chem. Soc.* **131**, 5873–5884 (2009).
3. Brun, M.A. *et al.* A semisynthetic fluorescent sensor protein for glutamate. *J. Am. Chem. Soc.* **134**, 7676–7678 (2012).
4. Brun, M.A. *et al.* Semisynthesis of fluorescent metabolite sensors on cell surfaces. *J. Am. Chem. Soc.* **133**, 16235–16242 (2011).
5. Masharina, A., Reymond, L., Maurel, D., Umezawa, K. & Johnsson, K. A fluorescent sensor for GABA and synthetic $GABA_B$ receptor ligands. *J. Am. Chem. Soc.* **134**, 19026–19034 (2012).
6. Lennard, L. Therapeutic drug monitoring of cytotoxic drugs. *Br. J. Clin. Pharmacol.* **52** (suppl. 1): 75S–87S (2001).
7. Keppler, A. *et al.* A general method for the covalent labeling of fusion proteins with small molecules *in vivo*. *Nat. Biotechnol.* **21**, 86–89 (2003).
8. Saito, K. *et al.* Auto-luminescent genetically-encoded ratiometric indicator for real-time Ca^{2+} imaging at the single cell level. *PLoS ONE* **5**, e9935 (2010).
9. Iwakura, M. & Nakamura, T. Effects of the length of a glycine linker connecting the N- and C-termini of a circularly permuted dihydrofolate reductase. *Protein Eng.* **11**, 707–713 (1998).
10. Jaffe, N. & Gorlick, R. High-dose methotrexate in osteosarcoma: let the questions surcease—time for final acceptance. *J. Clin. Oncol.* **26**, 4365–4366 (2008).
11. Al-Turkmani, M.R., Law, T., Narla, A. & Kellogg, M.D. Difficulty measuring methotrexate in a patient with high-dose methotrexate-induced nephrotoxicity. *Clin. Chem.* **56**, 1792–1794 (2010).
12. Kratz, A., Ferraro, M., Sluss, P.M. & Lewandrowski, K.B. Case records of the Massachusetts General Hospital. Weekly clinicopathological exercises. Laboratory reference values. *N. Engl. J. Med.* **351**, 1548–1563 (2004); erratum **351**, 2461.
13. Pollock, N.R. *et al.* A paper-based multiplexed transaminase test for low-cost, point-of-care liver function testing. *Sci. Transl. Med.* **4**, 152ra129 (2012).
14. Armstrong, V.W. & Oellerich, M. New developments in the immunosuppressive drug monitoring of cyclosporine, tacrolimus, and azathioprine. *Clin. Biochem.* **34**, 9–16 (2001).
15. Röhrig, C.H., Loch, C., Guan, J.Y., Siegal, G. & Overhand, M. Fragment-based synthesis and SAR of modified FKBP ligands: influence of different linking on binding affinity. *ChemMedChem* **2**, 1054–1070 (2007).
16. Patsalos, P.N. *et al.* Antiepileptic drugs—best practice guidelines for therapeutic drug monitoring: a position paper by the subcommission on therapeutic drug monitoring, ILAE Commission on Therapeutic Strategies. *Epilepsia* **49**, 1239–1276 (2008).
17. Valdes, R. Jr., Jortani, S.A. & Gheorghiade, M. Standards of laboratory practice: cardiac drug monitoring. National Academy of Clinical Biochemistry. *Clin. Chem.* **44**, 1096–1109 (1998).
18. Matsui, H. & Schwartz, A. Mechanism of cardiac glycoside inhibition of the $(Na^+\text{-}K^+)$-dependent ATPase from cardiac tissue. *Biochim. Biophys. Acta* **151**, 655–663 (1968).
19. Tinberg, C.E. *et al.* Computational design of ligand-binding proteins with high affinity and selectivity. *Nature* **501**, 212–216 (2013).
20. Terra, S.G., Washam, J.B., Dunham, G.D. & Gattis, W.A. Therapeutic range of digoxin's efficacy in heart failure: what is the evidence? *Pharmacotherapy* **19**, 1123–1126 (1999).
21. Smith, T.W. & Haber, E. Digoxin intoxication: the relationship of clinical presentation to serum digoxin concentration. *J. Clin. Invest.* **49**, 2377–2386 (1970).
22. Turner, A.P. Biosensors: sense and sensibility. *Chem. Soc. Rev.* **42**, 3184–3196 (2013).
23. Krishnamurthy, V.M., Semetey, V., Bracher, P.J., Shen, N. & Whitesides, G.M. Dependence of effective molarity on linker length for an intramolecular protein-ligand system. *J. Am. Chem. Soc.* **129**, 1312–1320 (2007).
24. Sawaya, M.R. & Kraut, J. Loop and subdomain movements in the mechanism of *Escherichia coli* dihydrofolate reductase: crystallographic evidence. *Biochemistry* **36**, 586–603 (1997).
25. Dubowchik, G.M. *et al.* 2-Aryl-2,2-difluoroacetamide FKBP12 ligands: synthesis and X-ray structural studies. *Org. Lett.* **3**, 3987–3990 (2001).
26. Schulz, M. & Schmoldt, A. Therapeutic and toxic blood concentrations of more than 800 drugs and other xenobiotics. *Pharmazie* **58**, 447–474 (2003).
27. Srivastava, D.K. *et al.* Structural analysis of charge discrimination in the binding of inhibitors to human carbonic anhydrases I and II. *J. Am. Chem. Soc.* **129**, 5528–5537 (2007).

Acknowledgments

This work was supported by École Polytechnique Fédérale de Lausanne, the Swiss National Science Foundation, the National Centre of Competence in Research Chemical Biology, and the Defense Threat Reduction Agency. We are grateful to T. Buclin, N. Widmer and L. Decosterd from the CHUV for helpful discussions.

Author contributions

R.G., A.S. and K.J. designed experiments, R.G. and A.S. performed experiments, A.S. and L.R. performed chemical synthesis and characterization of the sensor ligands, L.P. wrote software for image analysis, D.W. provided patient samples, and C.E.T. and D.B. provided DIG10.3. All of the authors contributed to the writing of the manuscript.

Competing financial interests

The authors declare competing financial interests: details accompany the online version of the paper.

Additional information

Supplementary information and chemical compound information is available in the online version of the paper. Reprints and permissions information is available online at http://www.nature.com/reprints/index.html. Correspondence and requests for materials should be addressed to K.J.

ONLINE METHODS

Chemical synthesis. Detailed procedures for SNAP-tag substrates **1**–**7** and **42** as well as other compounds can be found in **Supplementary Note 1**.

Sensor constructs. All sensor constructs were obtained from the previously described pET51b(+)-based construct SNAP-PP30-CLIP-HCA[4] using standard cloning techniques. The amino acid sequences of the described sensor proteins can be found in **Supplementary Figure 1**.

Sensor protein expression and labeling. The sensor proteins were expressed in the *E. coli* strain Rosetta-gami (DE3). Bacterial cultures in LB medium were grown at 37 °C to an $OD_{600\,nm}$ of 0.8, at which point the temperature was lowered to 16 °C, and 0.5 mM isopropyl β-D-thiogalactopyranoside (IPTG) was added. After 16 h, the cells were harvested by centrifugation and lysed by sonication. The cell extracts were cleared by centrifugation and purified in two steps using Ni-NTA (Qiagen) and Strep-Tactin (IBA) according to the suppliers' instructions. For SNAP-tag labeling, the sensor proteins were diluted to concentrations of 1 µM in buffer (50 mM HEPES, pH 7.2, 50 mM NaCl) containing 4 µM of the corresponding SNAP-tag substrate. After incubation at room temperature for 1 h, the labeled sensor constructs were used directly without further purification.

Titration curves. The labeled sensors were diluted to concentrations of 1 nM in 50 µl normal human serum (Merck Millipore) spiked with known concentrations of analyte in white nonbinding 96-well plates (Greiner Bio-One). After incubation at room temperature for 15–30 min, 50 µl Nano-Glo Luciferase Assay Substrate (Promega) diluted 100-fold in buffer (50 mM HEPES, pH 7.2, 50 mM NaCl) was added. Bioluminescence was measured on an EnVision Multilabel Reader (PerkinElmer). The signal was collected using an emission filter for Umbelliferone (wavelength: 460 nm, bandwidth: 25 nm) to record NanoLuc emission and a filter for Cy3 (wavelength: 595 nm, bandwidth: 60 nm) to record Cy3 or TMR emission. The ratio of donor and acceptor emission was plotted against the analyte concentration, and the data were fitted to a single binding isotherm (equation (1)) to obtain the c_{50} and maximum ratio change as previously described[2]. The c_{50} values and ratio changes are reported as the mean ± the s.d. from three independent experiments.

$$R = R_{zero} + \frac{R_{sat} - R_{zero}}{1 + \frac{c_{50}}{[MTX]}} \quad (1)$$

For sensors containing HCA, a twofold molar excess of $ZnCl_2$ was added to the purified protein. In contrast, for sensors containing DHFR, the cofactor NADPH was not added as it increases the affinity of both the intramolecular and free ligand, and the sensor would need to be incubated longer with the sample to reach equilibrium. As methotrexate absorbs in the blue region, high drug concentrations affect the observed ratio when titrations are performed in multiwell plates. For this reason, 200 µM was chosen as the highest concentrations in titrations of the sensor containing trimethoprim as intramolecular ligand, and a concentration of 1 mM was chosen for the sensor labeled with the methotrexate derivative. In titrations performed on paper, methotrexate absorbance is not an issue.

Emission spectra. Emission spectra were obtained essentially the same way as titration curves. The samples were prepared the same way except for the fact that a final sensor concentration of 10 nM was used. Spectra were measured on an Infinite M1000 spectrofluorometer (Tecan) with a step size of 1 nm, a bandwidth of 10 nm and an integration time of 50 ms.

Testing interference by absorbing substances. Titrations were performed as described above either using normal human serum or normal human serum spiked with additional 20 µM bilirubin (final concentration after addition of luciferase substrate: 10 µM). A sensor concentration of 10 nM was used. 3 µl from each well was then spotted onto pieces of Whatman No. 1 chromatography paper (GE Healthcare) that were produced using a standard hole punch, and these were put into empty wells of the same 96-well plate. The wells containing the paper were measured in the same way as the others.

Titrations in whole blood. Titrations in whole blood were performed in a similar way as in serum. The sensor protein was diluted in 25 µl bovine blood in heparin sodium (Antibodies Online Inc.) spiked with defined drug concentrations. 25 µl Nano-Glo Luciferase Assay Substrate diluted 50-fold in lytic Nano-Glo Luciferase Assay Buffer (Promega) was added. The samples were incubated for 3–5 min to allow for lysis of the red blood cells. 5 µl were spotted on the chromatography paper and analyzed as described above. As for the titrations in serum, a final sensor concentration of 50 nM was used.

Detection using a digital camera. Black circles in the shape of the wells of a 96-well plate were printed onto Whatman No. 1 chromatography paper (GE Healthcare) using a Xerox Phaser 8560 solid ink printer. The paper was then heated in an oven at 90 °C for 5–10 min until the black circles were well visible from the opposite side.

Solutions in multiwell plates were prepared the same way as described above for titration curves except for the fact that final sensor concentrations between 5 nM and 50 nM were used. 3–5 min after the addition of the luciferase substrate, 5 µl from each solution was spotted in the center of the circles printed on the paper. After 1–2 min, a picture of the paper was taken using a digital camera through a hole in a polystyrene ice box to prevent light from the environment to disturb the measurement. The white balance of the camera was set in such a way that the red and blue spots were well distinguishable.

Final sensor concentrations of 50 nM for the methotrexate LUCID and 25 nM for the topiramate and cyclosporin A LUCIDs were used. The pictures were taken using a Canon PowerShot SX150 IS digital camera with an exposure time of 15 s, an F value of 3.4 and an ISO value of 1,600, and the focus was set manually to 10–15 cm. Because of the low c_{50} values, 5 nM was used as a final concentration for the tacrolimus/sirolimus LUCID as well as for the digoxin LUCID. Because of the lower light intensity, a Canon PowerShot G1X digital camera with an exposure time of 60 s, an F value of 2.8 and an ISO value of 5,000 was used, with the focus set manually to the lowest possible setting.

To process the images, a java servlet based on ImageJ[28] was developed. In a first step, the parts of the pictures corresponding to spots were isolated. Because of reduced contrast in the pictures and the change of color, it was found that the most suitable procedure to create a binary mask was to split the color image in HSB components and apply Li's minimum cross entropy thresholding method on the brightness component[29]. The resulting regions of interest (ROIs) were filtered out on the basis of the surface area. To calculate the average content of red and blue of each subimage, a red and blue histogram was generated, and a weighted mean was taken as the average respective red and blue content. The source code of the java servlet is available in **Supplementary Note 2**.

Measurement of methotrexate in patient samples using LUCIDs. Thirty serum samples from patients undergoing treatment with methotrexate were obtained from the University Hospital of Lausanne (CHUV). 5 µl of a stock solution containing 500 nM labeled sensor was added to 25 µl of the patient samples. After incubation at room temperature for at least 15 min, 20 µl Nano-Glo Luciferase Assay Substrate (Promega) diluted 100-fold in buffer (50 mM HEPES, pH 7.2, 50 mM NaCl) was added, and detection using a digital camera was carried out as described above.

Up to 20 samples were measured in parallel. In addition to the samples, a reference curve consisting of 16 samples of normal human serum spiked with known concentrations of methotrexate was included in each experiment. Equation (1) was used to fit the ratios obtained from the reference samples and to calculate the concentrations of the samples on the basis of the measured ratios. Interassay coefficients of variation for each sample were calculated by dividing the s.d. from three independent measurements by the mean. As no clear dependence on the mean concentration was observed, the average coefficient of variation was determined.

The experiments were done blindly, i.e., without previous knowledge of the results obtained by the reference method. All of the experiments involving samples from patients were approved by the Commission cantonale (VD) d'éthique de la recherche sur l'être humain.

Measurement of methotrexate in patient samples using a fluorescence polarization immunoassay. Samples from patients were measured at the University Hospital of Lausanne (CHUV) on a TDxFLx using the Methotrexate II assay (Abbott) according to the supplier's instructions.

28. Schneider, C.A., Rasband, W.S. & Eliceiri, K.W. NIH Image to ImageJ: 25 years of image analysis. *Nat. Methods* **9**, 671–675 (2012).
29. Li, C.H. & Tam, P.K.S. An iterative algorithm for minimum cross entropy thresholding. *Pattern Recognit. Lett.* **19**, 771–776 (1998).

doi:10.1038/nchembio.1554